

Supplemental Experimental Procedures

Drosophila strains and culture

Unless otherwise indicated, flies were raised at low density on standard cornmeal/molasses/agar medium at 25°C. *y w* flies isogenic for the second and third chromosomes were used as wild type and for P element transformation. The following mutant and transgenic stocks were used: *Atg1^{A3D}*, Hsp70-GFP-*Atg8a^{6A}*, and Hsp70-GFP-*Atg8b^{6B}* [1], *Atg8a^{KG07569}*, *Aut1^{EY08396}* (obtained from Bloomington Drosophila Stock Center), *gig¹⁰⁹* [2], *gig¹⁹²* [3], *Pdk1⁵* [4], *Tor^{AP}* [5], *Df(3L)Cat* [6], Cg-GAL4 [7], fb-GAL4 [8], GMR-GAL4¹² [9], Hsp70-GAL4 [10], UAS-*Atg1^{GS10797}* (obtained from Kyoto Drosophila Genetic Resource Center), UAS-*Aut1* [11], UAS-DIAP1.H (B. Hay), UAS-p35 [12], UAS-*Rheb^{AV4}* [13], UAS-*Rheb^{EP50.084-loxP}* [14].

Electron microscopy

24-48 hours after hatching, 50 or fewer larvae were transferred to a vial containing fresh fly food supplemented with yeast paste. 24 hours later, larvae were dissected immediately (fed) or placed in vials containing 20% sucrose for 3-4 hours prior to dissection (starved). Larvae were then bisected in PBS and inverted carcasses were fixed overnight at 4°C in 2% paraformaldehyde, 4% glutaraldehyde, 2% sucrose in 100 mM phosphate buffer; rinsed in 3% sucrose, 100 mM phosphate buffer; and post-fixed in 2% OsO₄ in 100 mM phosphate overnight at 4°C. Carcasses were dehydrated in ethanol, and fat body was dissected and embedded in Polybed 812. 60 nm sections were cut and collected on uncoated 200 mesh copper grids. Sections were stained in 3% aqueous uranyl acetate for 20 min, rinsed, stained with Sato triple lead stain for 3 min, rinsed, and air dried. Stained sections were viewed on an FEI CM-12 transmission electron microscope.

Lysotracker staining

Fat body from fed or starved larvae (as above) or larvae fed for 24 hr on 10 μM rapamycin in fly medium was dissected in PBS and incubated for 2 min in 100 μM LysoTracker Red DND-99 (Molecular Probes) in PBS with 1 μM Hoechst 33342 or 1 μg/mL 4',6-diamidino-2-phenyl-indole (DAPI). Portions of

fat body were transferred to PBS on glass slides, covered, and immediately photographed live. Lysotracker density was calculated as in [1], using 5 images of each genotype (average area quantitated = 8040 μm^2), and normalized to the values of starved wild type animals.

Immunohistochemistry

Unless otherwise indicated, larvae were dissected in PBS 48-96 hr after hatching, then fixed for 20-30 min (imaginal discs) or overnight at 4°C (fat body) in 3.7% formaldehyde in PBS or PBTx (PBS plus 0.1% Triton-X-100 +/- 0.1% sodium deoxycholate) and rinsed in PBTx. Antibody stained samples were blocked for 20 min (imaginal discs) or 2 hr (fat body) in 5% normal goat serum in PBTx (PBTxG), stained overnight at 4°C with primary antibody in PBTxG, washed in PBTx, incubated overnight at 4°C with secondary antibody in PBTxG, and washed in PBTx and PBS. Alpha spectrin (3A9) antibody (Developmental Studies Hybridoma Bank) was used at 1:100 dilution. Active caspase-3 (CM1) antibody (BD Biosciences) was used at 1:10,000 dilution, 24 hr after 1 hr heat shock. FOXO (3015) antibody [15] was used at 1:300 dilution. Texas Red conjugated goat anti-rabbit or anti-mouse was used as secondary antibody at 1:500 dilution. GFP-Atg8 expression was induced as described [1], except Lysotracker staining of these lines was performed after 3 min fixation as in [16], and rescue of Atg8a mutant was achieved with an additional heat shock 24 hr prior to dissection. Alexa-Fluor 586 phalloidin (Molecular Probes) was used at a concentration of 5 units/mL in PBTx, overnight at 4°C. TUNEL staining was performed using the Roche In Situ Cell Death Detection Kit (TMR Red) 45 hr after 30 min heat shock. 1 μM Hoechst 33258 or 1 $\mu\text{g/mL}$ DAPI was used to stain nuclei.

For Western blot analysis, Hsp70-GAL4 driven transgene overexpression was induced as above. Fat body or wing discs dissected from late third instar larvae or entire animals were boiled in 2x sample buffer, and run on 10% polyacrylamide gel. S6K-phospho-T398 antibody (Cell Signaling Technology) and S6K antibody (gift of T. Radimerski and G. Thomas) were used at 1:1000 dilution. GFP antibody (Torrey Pines Biolabs) was used at 1:2000 dilution. Beta tubulin (E7) antibody (Developmental Studies Hybridoma Bank) was used at 1:10,000 dilution.

UAS-Atg1 lines

Drosophila Atg1 cDNA (AT02023) was cloned into pUAST as an EcoRI/XhoI fragment to generate the UAS-Atg1 lines. The site-directed Atg1^{K38Q} mutant was generated in the following manner: the Atg1 cDNA was PCR amplified from the Cys39 codon (base 115 of the ORF) to the SmaI restriction site (base 1305), adding an adenine to generate an NsiI site, as well as an EcoRI site, at the 5' end; and an XbaI site at the 3' end. This PCR product was cloned into pBlueScriptII KS+. The Atg1 cDNA was then PCR amplified from the beginning of the EST clone to the Ile37 codon (base 111), adding a TG linker and NsiI site at the 3' end to replace Lys38 with Gln, and cloned into the plasmid described above. The 3' end of Atg1 was cloned from UAS-Atg1 into the resulting plasmid as a SmaI/XbaI fragment, and the full length Atg1^{K38Q} cloned into UAST as an EcoRI/XhoI fragment. The UAS-Atg1^{K38Q} line used in this study (13A) contains two independent insertions of UAS-Atg1^{K38Q}.

P element excision

P element EY08396 is inserted in the 5' UTR of *Atg3/Aut1*, 30 bases upstream of the start of the *Atg3* coding region. Deletions resulting from excision of this element were generated with transposase and identified by PCR as described [5]. The deletion used in this study (*Aut1*¹⁰) eliminates 838 bases upstream of the EY08396 insertion site, including the first and part of the second exon of the neighboring *Nufip* gene, and results in lethality at the late larval/early prepupal period. P element KG07569 is a viable insertion in codon 28 of the *Atg8a* ORF. A precise excision (ex3) of this element was generated and identified as for *Atg3* deletions.

Microscopy

Live, LysoTracker stained tissues were photographed on a Zeiss Axioscope 2 fluorescent microscope. Adult eyes were photographed on a Zeiss Stemi SV 11 dissecting microscope. Confocal images of all other tissues were photographed on a Zeiss Axioplan 2 fluorescent microscope with an Atto Instruments CARV spinning disc unit.

Supplemental References

1. Scott, R.C., Schuldiner, O., and Neufeld, T.P. (2004). Role and regulation of starvation-induced autophagy in the *Drosophila* fat body. *Dev Cell* 7, 167-178.
2. Meinertzhagen, I.A. (1994). The early causal influence of cell size upon synaptic number: the mutant *gigas* of *Drosophila*. *J Neurogenet* 9, 157-176.
3. Ito, N., and Rubin, G.M. (1999). *gigas*, a *Drosophila* homolog of tuberous sclerosis gene product-2, regulates the cell cycle. *Cell* 96, 529-539.
4. Rintelen, F., Stocker, H., Thomas, G., and Hafen, E. (2001). PDK1 regulates growth through Akt and S6K in *Drosophila*. *Proc Natl Acad Sci U S A* 98, 15020-15025.
5. Zhang, H., Stallock, J.P., Ng, J.C., Reinhard, C., and Neufeld, T.P. (2000). Regulation of cellular growth by the *Drosophila* target of rapamycin *dTOR*. *Genes Dev* 14, 2712-2724.
6. Mackay, W.J., and Bewley, G.C. (1989). The genetics of catalase in *Drosophila melanogaster*: isolation and characterization of acatalasemic mutants. *Genetics* 122, 643-652.
7. Asha, H., Nagy, I., Kovacs, G., Stetson, D., Ando, I., and Dearolf, C.R. (2003). Analysis of Ras-induced overproliferation in *Drosophila* hemocytes. *Genetics* 163, 203-215.
8. Gronke, S., Beller, M., Fellert, S., Ramakrishnan, H., Jackle, H., and Kuhnlein, R.P. (2003). Control of fat storage by a *Drosophila* PAT domain protein. *Curr Biol* 13, 603-606.
9. Freeman, M. (1996). Reiterative use of the EGF receptor triggers differentiation of all cell types in the *Drosophila* eye. *Cell* 87, 651-660.
10. Halfon, M.S., Kose, H., Chiba, A., and Keshishian, H. (1997). Targeted gene expression without a tissue-specific promoter: creating mosaic embryos using laser-induced single-cell heat shock. *Proc Natl Acad Sci U S A* 94, 6255-6260.
11. Juhász, G., Csikós, G., Sinka, R., Erdélyi, M., and Sass, M. (2003). The *Drosophila* homolog of Aut1 is essential for autophagy and development. *FEBS Lett* 543, 154-158.
12. Zhou, L., Schnitzler, A., Agapite, J., Schwartz, L.M., Steller, H., and Nambu, J.R. (1997). Cooperative functions of the *reaper* and *head involution defective* genes in the programmed cell death of *Drosophila* central nervous system midline cells. *Proc Natl Acad Sci U S A* 94, 5131-5136.

13. Patel, P.H., Thapar, N., Guo, L., Martinez, M., Maris, J., Gau, C.L., Lengyel, J.A., and Tamanoi, F. (2003). *Drosophila* Rheb GTPase is required for cell cycle progression and cell growth. *J Cell Sci* 116, 3601-3610.
14. Stocker, H., Radimerski, T., Schindelholz, B., Wittwer, F., Belawat, P., Daram, P., Breuer, S., Thomas, G., and Hafen, E. (2003). Rheb is an essential regulator of S6K in controlling cell growth in *Drosophila*. *Nat Cell Biol* 5, 559-566.
15. Puig, O., Marr, M.T., Ruhf, M.L., and Tjian, R. (2003). Control of cell number by *Drosophila* FOXO: downstream and feedback regulation of the insulin receptor pathway. *Genes Dev* 17, 2006-2020.
16. Rusten, T.E., Lindmo, K., Juhász, G., Sass, M., Seglen, P.O., Brech, A., and Stenmark, H. (2004). Programmed autophagy in the *Drosophila* fat body is induced by ecdysone through regulation of the PI3K pathway. *Dev Cell* 7, 179-192.

Supplemental Figure legends

Supplemental Figure S1. Atg1 rescue and additional LysoTracker staining in fat body.

(A) Transgenic Atg1 partially rescues lethality of *Atg1* null mutants. *Atg1* null mutants (control) result in fully penetrant pupal lethality. Low levels of Atg1 expression from uninduced heat shock promoter (*Atg1*) results in a mean rescue of 34% of expected flies to viability, whereas expression of a kinase dead mutant of Atg1 (*Atg1*^{K38Q}) results in only 4% mean rescue. * indicates a significant difference from the control: $p = 0.0011$; ** indicates a significant difference from wild type Atg1 $p = 0.0029$.

(B-C) Transgenic Atg1 rescues starvation-induced autophagy. Fat body from well-fed *Atg1* null mutant larvae expressing Atg1 from uninduced heat shock promoter show no detectable autophagy (B), whereas starvation of these animals induces autophagy (C).

(D) Kinase defective Atg1 does not rescue starvation-induced autophagy in *Atg1* null mutants.

(E) Clonal overexpression of endogenous Atg1 (GFP positive cells) causes cell-autonomous induction of LysoTracker staining. Inset shows LysoTracker channel, with clonal boundaries outlined in yellow.

(F) Expression of kinase-defective Atg1 cell autonomously inhibits induction of LysoTracker staining induced by rapamycin treatment.

(G) Quantitation of LysoTracker staining. † indicates no significant difference from wild type (or *Atg1^{-/-}*): $p > 0.3$; *** indicates a significant difference from *Atg1^{-/-}*: $p = 0.0027$; ††† indicates no significant difference from *Atg1^{-/-}*: $p = 0.84$.

Scale bars represent 10 μm . Nuclei are marked in blue. Error bars indicate SD.

Genotypes: (A) No Rescue: *Hsp70-GAL4 Atg1 ^{Δ 3D}/Atg1 ^{Δ 3D}*. *Atg1*: As in panels B & C. *Atg1^{K38Q}*: As in panel D. (B-C) *Hsp70-GAL4 Atg1 ^{Δ 3D}/UAS-Atg1^{6B} Atg1 ^{Δ 3D}*. (D) *Hsp70-GAL4 Atg1 ^{Δ 3D}/UAS-Atg1^{KQ13A} Atg1 ^{Δ 3D}*. (E) *hsflp/+; Act>CD2>GAL4 UAS-GFP/UAS-Atg1^{GS10797}*. (F) *hsflp/+; Act>CD2>GAL4 UAS-GFP/UAS-Atg1^{KQ13A}*. (G) As in panels B, C, & D.

Supplemental Figure S2. Overexpression of *Atg1* in the eye.

(A-C) *Atg8a* levels and localization in eye disc cells overexpressing *Atg1*. In control animals, heat shock-driven GFP-*Atg8a* expression is uniform across the eye disc field (A). GMR-GAL4-driven expression of *Atg1* in cells posterior to the morphogenetic furrow results in increased levels of GFP-*Atg8a* relative to control cells anterior to the furrow (B). Overexpression of *Atg1* behind the morphogenetic furrow (arrow) also results in punctate localization of GFP-*Atg8a* (C). (A) shows two representative confocal sections. Discs are shown anterior rightward.

(D) Flies overexpressing *Atg1* in the eye disc show increased lethality, but this lethality can be rescued by co-overexpression of p35, DIAP1, or kinase defective *Atg1*. ** indicates a significant difference from *Atg1* alone: $p < 0.03$. Error bars indicate SD.

(E) Western blot showing a greater than 2.4-fold increase in GFP-*Atg8b* in wing discs overexpressing *Atg1*.

(F-J) *Atg1* overexpression in the adult eye. Overexpression of *Atg1* (G) greatly reduces the size of the adult eye, as compared with a wild type control (F). Co-overexpression of DIAP1 (H) or kinase defective *Atg1* (I) rescues this size defect. Overexpression of kinase inactive *Atg1* has little effect on the size or patterning of the adult eye (J).

Scale bars represent 10 μm in panels (A-C) and 100 μm in panels (E-I).

Genotypes: (A, C) *Hsp70-GFP-Atg8a^{6A}/+*; *GMR-GAL4¹² UAS-Atg1^{6A}/+*. (B) *Hsp70-GFP-Atg8a^{6A}/+*; *GMR-GAL4¹²/+*. (D) Atg1: *GMR-GAL4¹² UAS-Atg1^{6A}/+*. Atg1 p35: *GMR-GAL4¹² UAS-Atg1^{6A}/+*; *UAS-p35/+*. Atg1 DIAP1: *GMR-GAL4¹² UAS-Atg1^{6A}/+*; *UAS-DIAP1.H/+*. Atg1 Atg1K38Q: *GMR-GAL4¹² UAS-Atg1^{6A}/+*; *UAS-Atg1^{KQ13A}/+*. (E) Control: *Hsp70-GFP-Atg8b^{6B}/MS1096-GAL4*. Atg1: *Hsp70-GFP-Atg8b^{6B}/MS1096-GAL4*; *UAS-Atg1^{6B}/+*. (F) *GMR-GAL4¹²/+*. (G) *GMR-GAL4¹²/+*; *UAS-Atg1^{6B}/+*. (H) *GMR-GAL4¹²/+*; *UAS-Atg1^{6B}/UAS-DIAP1.H*. (I) *GMR-GAL4¹²/+*; *UAS-Atg1^{6B}/UAS-Atg1^{KQ13A}*. (J) *GMR-GAL4¹²/+*; *UAS-Atg1^{KQ13A}/+*.

Supplemental Figure S3. Atg3 and Atg8a mutants disrupt Atg1-induced phenotypes.

(A-D) *Atg8a* mutants disrupt starvation-induced autophagy. In wild-type animals, starvation leads to robust induction of autophagy (A), which is significantly reduced by disruption of *Atg8a* (B). This deficiency is rescued by ubiquitous expression of GFP-*Atg8a* (C) and by precise excision of the P element (D).

(E-H) *Atg3* is required for autophagy. Starvation-induced autophagy is strongly inhibited by mutation of *Atg3* (E); this defect is rescued by transgenic *Atg3* (F). Similarly, heat shock-induced overexpression of *Atg1* results in induction of autophagy (G), and mutation of *Atg3* inhibits this induction of autophagy (H).

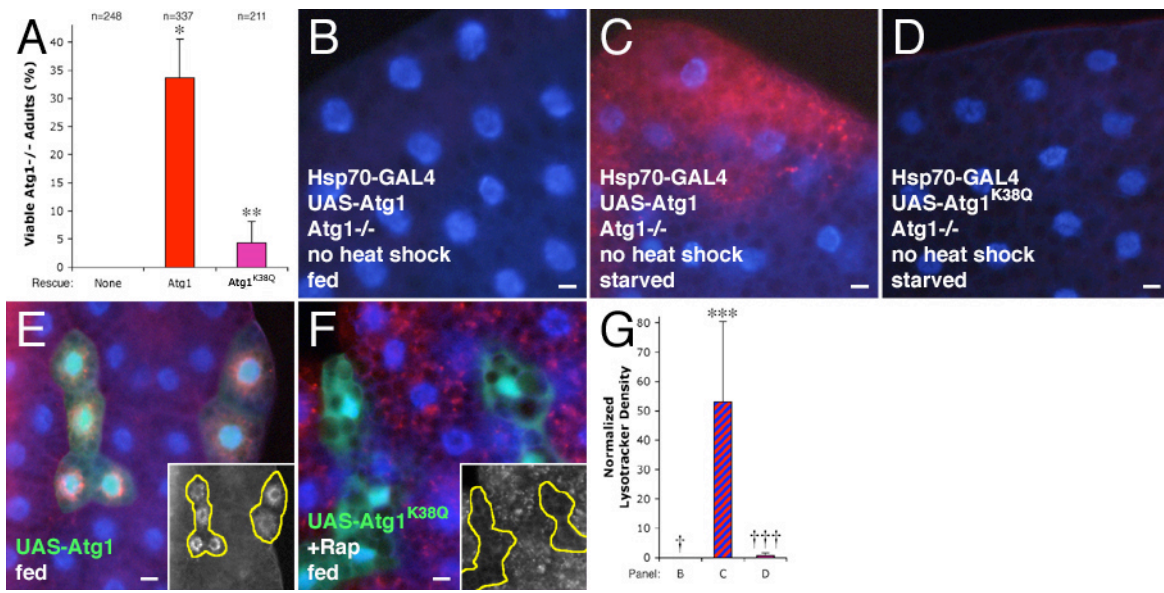
(I-J) Suppression of cell death by mutation of *Atg3*. Constitutive overexpression of *Atg1* in the fat body induces DNA fragmentation by TUNEL staining (arrowheads) in 17% of cells (I). This effect is reduced by 94% in *Atg3* mutants (J).

(K) Quantitation of Lysotracker staining. * indicates a significant difference from wild type: $p = 0.0006$; **** indicates a significant difference from *Atg8a*⁻: $p = 0.010$ (and no significant difference from wild type: $p > 0.27$); ***** indicates a significant difference from *Atg3*^{-/-}: $p = 0.0003$; ** indicates a significant difference from *Atg1* overexpression alone: $p < 0.0001$.

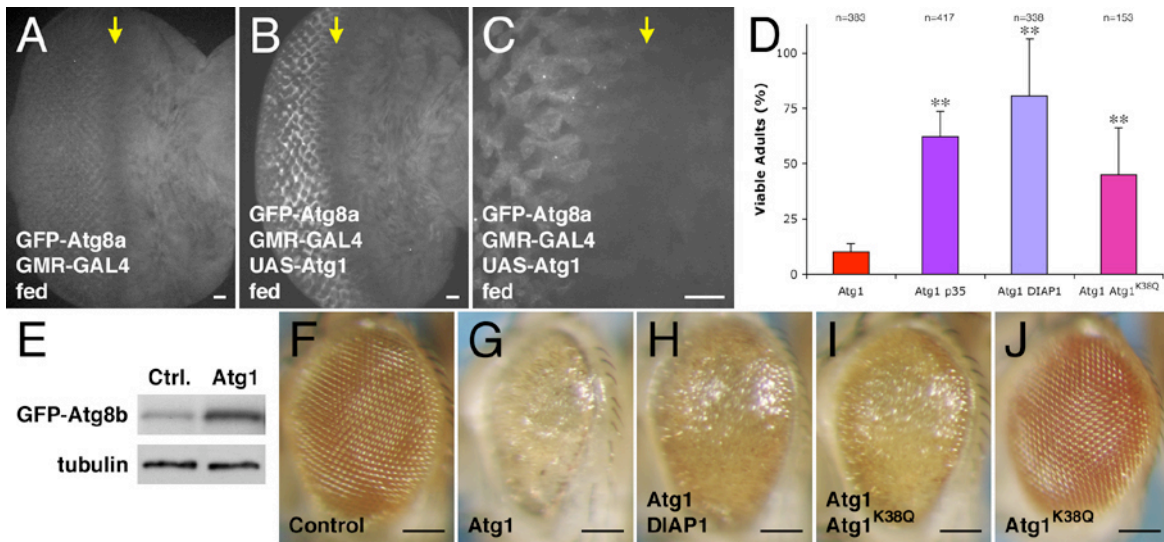
Scale bars represent 10 μ m. Nuclei are marked in blue. Error bars indicate SD.

Genotypes: (A) +/+ . (B) *Atg8a^{KG07569}/Y*. (C) *Atg8a^{KG07569}/Y*; *Hsp70-GFP-Atg8a³⁴/+*. (D) *Atg8a^{ex3}/Y*. (E) *Aut1¹⁰/Df(3L)Cat*. (F) *Cg-GAL4/UAS-Aut1*; *Aut1¹⁰/Df(3L)Cat*. (G) *Hsp70-GAL4/UAS-Atg1^{6B}*.

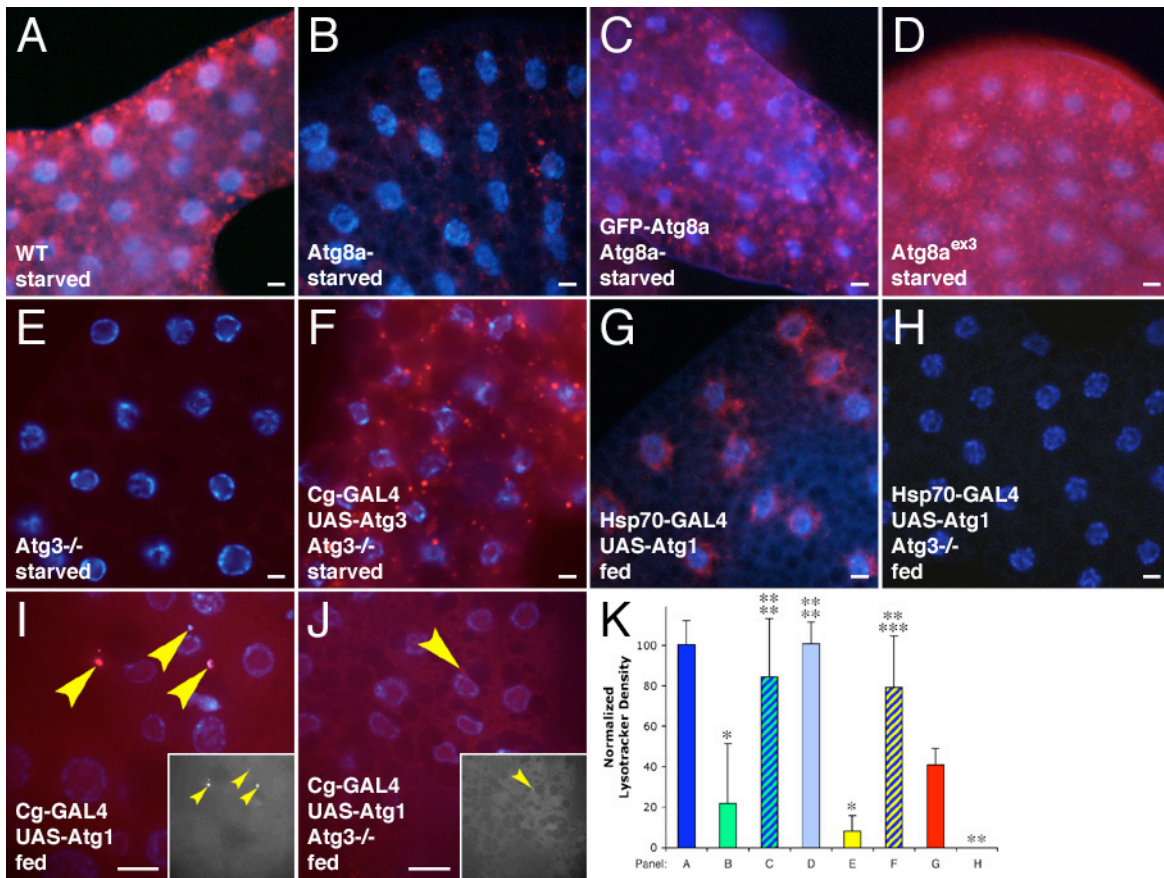
(H) *Hsp70-GAL4 Aut1¹⁰/UAS-Atg1^{6B} Df(3L)Cat*. (I) *Cg-GAL4/+; UAS-Atg1^{GS10797}/+*. (J) *Cg-GAL4/+; UAS-Atg1^{GS10797} Atg3¹⁰/Atg3¹⁰*. (K) As in panels A-H.



Supplemental Figure S1



Supplemental Figure S2



Supplemental Figure S3